Chemical Geology 277 (2010) 336–344

Contents lists available at ScienceDirect

Chemical Geology

journal homepage: www.elsevier.com/locate/chemgeo

A detailed $^{87}SR/^{86}SR$ isotopic curve for the mid-Cincinnatian (Upper Katian–Lower Hirnantian, Upper Ordovician), NE North American Shelf (Ontario, Canada) transition to the Hirnantian glaciation

R. Hannigan [a], M.E. Brookfield [b,*], A.R. Basu [c]

[a] Environmental Earth and Ocean Sciences, University of Massachusetts at Boston, 100 Morrissey Blvd, Boston, MA 02125, USA
[b] Institute of Earth Sciences, Academia Sinica, P.O. Box 1-55, Nankang, Taipei 11529, Taiwan
[c] Department of Earth and Environmental Sciences, University of Rochester, Rochester, NY 14627, USA

ARTICLE INFO

Article history:
Received 13 November 2009
Received in revised form 14 August 2010
Accepted 17 August 2010

Editor: J.D. Blum

Keywords:
Sr
Isotopes
Ontario
Cincinnatian
Ordovician
Glaciation

ABSTRACT

We examined the Sr-isotopic composition of one species of well-preserved brachiopod species from the mid-Cincinnatian (Upper Katian–Lower Hirnantian, Upper Ordovician) in closely spaced samples from one borehole on the western shelf of the Upper Ordovician Appalachian low latitude retroarc basin in southwestern Ontario. The section spans the transition from passive margin carbonate ramp through anoxic shales into foredeep orogenic clastics and encompasses the transition into the late Ordovician glaciation. The primary nature of the Sr-isotopic composition of the shells shows several stable Sr-isotopic excursions that refine the Upper Ordovician Sr-isotopic curve, and indicate several marked changes that may be related to the competing influences of island arc and ophiolite nappe emplacement and erosion, increasing continental crust erosion during the Taconic orogeny and the glacio-eustatic drop in sea-level related to the onset of the late Ordovician Hirnantian glaciation. These changes begin with low Sr isotope ratios (~0.7090) consistent with the overall trends but the ratios then change to much more positive, reaching high Sr isotope ratios (~0.7084) not elsewhere attained until the end Silurian. These and other minor fluctuations are attributed to periodic increases in Sr isotope ratios in the semi-isolated Taconic retroarc basin caused by rivers draining unroofing continental thrust sheets and earlier Ordovician carbonate cover rocks, with their higher Sr isotope ratios, together with increased continental erosion during regression associated with the onset of the main phase of the late Ordovician glaciation and possible glacial/interglacial phases.

1. Introduction

The strontium (Sr) isotope composition of past seawater, as determined from marine carbonate shells and rocks has been used as a proxy for tectonic evolution because $^{87}Sr/^{86}Sr$ variations mainly show the balance between river input from continents and mantle input from submarine hydrothermal systems (Veizer and Compston, 1974; Spooner, 1976; Burke et al., 1982; Veizer, 1989; Dennison et al., 1998; Veizer et al., 1999; McArthur et al., 2001). In addition, such variations are used as correlation tools, especially in poorly fossiliferous sediments (Elderfield, 1986; McArthur, 1994). However, $^{87}Sr/^{86}Sr$ analysis of marine sediments has been used not only for chronostratigraphy but also to compare Sr-isotopic ratios with sea-level patterns, times of orogeny and glaciation, and taxonomic diversity through time and determine their relationships (Purdy, 2008). For this, it is therefore necessary to determine Sr-isotopic fluctuations during the Phanerozoic as accurately and precisely as possible. We report our $^{87}Sr/^{86}Sr$ ratios to six decimal places to follow conventional practice, though this violates significance rules in our study (see Table 1): also, in some comparisons, we can only use the precision used in some older studies (often four decimal places).

Variations in $^{87}Sr/^{86}Sr$ ratios in marine sediments are driven by variations in the contribution of high (continental) and low (oceanic) $^{87}Sr/^{86}Sr$ ratio sources (Spooner, 1976). Excursions in marine $^{87}Sr/^{86}Sr$ ratios towards higher values reflect changes in the flux of radiogenic Sr from the continents caused by increased erosion from continents during marine regressions (either glacial or non-glacial) and/or orogenic phases, with the high current oceanic $^{87}Sr/^{86}Sr$ ratio (~0.7092) the result of both (DePaolo, 1986; Richter et al., 1992; France-Lanord et al., 1993): and conversely lower values reflect hydrothermal flux of less radiogenic Sr from the ocean ridges and oceanic arcs during more rapid spreading, and burial of continental sources by marine transgressions (Stille and Shields, 1997; Dennison et al., 1998; Jones and Jenkyns, 2001); though other factors have to be taken into account as well, such as erosion of island arcs, emplaced ophiolites and flood basalts (Jones and Jenkyns, 2001; Young et al., 2009). For example, most large rivers draining large continental areas have $^{87}Sr/^{86}Sr$ ratios between 0.7100 and 0.7200, whereas rivers draining Cenozoic island arcs have an

* Corresponding author.
E-mail addresses: Robyn.Hannigan@umb.edu (R. Hannigan), mbrookfi@hotmail.com (M.E. Brookfield), asish.basu@rochester.edu (A.R. Basu).

0009-2541/$ – see front matter © 2010 Elsevier B.V. All rights reserved.
doi:10.1016/j.chemgeo.2010.08.016

Table 1
Sr isotopic ratios and Sr and Mn contents for brachiopods *Paucicrura rogata* (Sardeson, 1892) from the Swift Current core. Sr isotope ratios have errors of ±0.000029 (2σ, ± 0.006%) which limits significant decimals to 5 (see Methods section), though the sixth decimal place is given in the table to follow conventional reporting.

Analysis number	Sample notation	[Sr] ppm	[Mn] ppm	$^{87}Sr/^{86}Sr$ ±0.000029
1	Tr-45-ON	1348	52	0.707912
2	Tr-41-ON	1963	43	0.707861
3	Tr-40-ON	2243	22	0.707923
4	Tr-35-ON	2339	85	0.707887
5	Tr-33-ON	1789	42	0.707912
6	CB-32-ON	1137	76	0.707878
7	CB-28-ON	1200	35	0.707851
8	CB-25-ON	1921	46	0.707882
9	CB-21-ON	1302	58	0.707907
10	CB-14-ON	1441	62	0.707824
11	CB-10-ON	1224	74	0.708091
12	CB-8.5-ON	1733	95	0.708012
13	MD-8.2-ON	1432	101	0.708121
14	MD-7.8-ON	1100	86	0.708218
15	MD-7.2-ON	1559	23	0.708248
16	MD-6.7-ON	1833	46	0.708321
17	MD-6-ON	1612	48	0.708333
18	MD-5.5-ON	1403	52	0.708329
19	MD-5.2-ON	1387	72	0.708353
20	MD-5-ON	1236	92	0.708451
21	MD-4.5-ON	1242	94	0.708419
22	MD-4-ON	1264	95	0.708363
23	MD-3.5-ON	1245	101	0.708382
24	MD-3-ON	1268	87	0.708354
25	MD-2.5-ON	1333	105	0.708309
26	MD-2-ON	1369	105	0.708259
27	MD-1-ON	1349	111	0.708353
28	MD-0-ON	1243	84	0.708507

average $^{87}Sr/^{86}Sr$ ratio of 0.7076 (Japan) to 0.7083 (Indonesia) (Palmer and Edmond, 1989). Ophiolites emplacement is frequently closely followed by massive erosion, for example in Oman (with pervasive hydrothermal alteration — $^{87}Sr/^{86}Sr$ ~0.70514) (Brookfield, 1977; Kawahata et al., 2001). Ophiolites, like the huge Bay of Islands ophiolite, Newfoundland (still 100×25 km in area) (Williams, 1975), with hydrothermally altered variable $^{87}Sr/^{86}Sr$ ratios between 0.70254 to 0.70804 (Jacobsen and Wasserburg, 1979), and emplaced in the latest Middle Ordovician, supplied ophiolitic detritus to the Upper Ordovician Taconic basin (Nelson and Casey, 1979).

Open ocean $^{87}Sr/^{86}Sr$ ratios are globally very uniform because of the long oceanic residence time of Sr (2–5 Ma), combined with a relatively short (<1000 years) oceanic mixing rate, even in recent semi-isolated seas, such as the Arctic and Mediterranean (Veizer, 1989; McArthur, 1994; Winter et al., 1997; Flecker and Ellamb, 2006). Hudson Bay, with a surface salinity of 24‰ to 29‰ has a normal ocean Sr isotope ratio of 0.709249 ± 0.000012 in its southern part furthest from the Hudson Strait (Capo and DePaolo, 1992). Further study is needed, however, since only 'subsurface' was used to locate the 2 samples analyzed, the Bay has a pronounced estuarine circulation with fresh water exiting over seawater entering, and salinities vary from <30‰ at the surface to 33‰ below 60 m (only slightly less than normal marine of 35‰) in the same area as the samples were collected (Prinsberg, 1986). The Baltic Sea, which is closer in shape to the Taconic basin (Maslowski and Walczowski, 2002; Gustafsson and Omstedt, 2009) has $^{87}Sr/^{86}Sr$ ratios varying from 0.709319 to 0.709207 from surface to 225 m in its southern part (Andersson et al., 1992). $^{87}Sr/^{86}Sr$ ratios of oceans and enclosed to semi-enclosed seas, however, need not be uniform, depending on the relative isolation of the latter and their oceanography (Stille et al., 1992; Bahr et al., 2008; Vasiliev et al., 2010).

The $^{87}Sr/^{86}Sr$ ratios through the Paleozoic have been established through studies over many years (Veizer and Compston, 1974; Burke et al., 1982; Veizer, 1989; Dennison et al., 1998; Veizer et al., 1999; McArthur et al., 2001). Yet many sections of the curve, like the Upper Ordovician show very wide spreads in apparently contemporary sediments. Furthermore, the scatter of contemporary values is much greater than in the earlier Upper Cambrian and Silurian, especially in the Upper Ordovician (Shields et al., 2003)(Fig. 1).The Upper Ordovician begins with a sharp decrease in $^{87}Sr/^{86}Sr$ ratios, among the most rapid in the entire Phanerozoic, to less radiogenic values (from ~0.7087 to ~0.7078) (Young et al., 2009) and ends with a sharp increase in $^{87}Sr/^{86}Sr$ ratios which then gradually increase during the Silurian (from ~0.7078 to 0.7083) (Ruppel et al., 1996; Veizer et al., 1999; Shields et al., 2003) similar to, but less marked than, the shift observed in the Cenozoic (Koepnick et al., 1985; Palmer and Elderfield, 1985). It is curious that the end Cambrian to Middle Ordovician part of the curve mimics in reverse, the early Miocene to Recent curve over the same 20 million year time interval, and with the same $^{87}Sr/^{86}Sr$ ratios (DePaolo, 1986). Like the Cenozoic, the latest Ordovician to Silurian increase has been attributed to marine regression, mountain building, and cooling, and hence increased erosion during orogeny and the onset and climax of ice ages (Palmer and Elderfield, 1985; Qing et al., 1998; Shields et al., 2003), though even the relative influence of different fluxes in the Cenozoic Sr-isotopic record is debatable (Hess et al., 1986; France-Lanord et al., 1993). The Neogene rapid rise in seawater $^{87}Sr/^{86}Sr$ ratios (DePaolo, 1986) can, at least partly, be attributed to the Miocene metamorphism and anatexis of Himalayan metasedimentary rocks, southward displacement and massive erosion of the nappes of the high Himalaya, involving removal of at least 130 km width of a 20 km thick part of the former Indian inner passive margin and its basement (Brookfield, 1993; Harris, 1995), a feature also of the Taconic orogeny (Bradley, 1989).The scatter of $^{87}Sr/^{86}Sr$ values within individual Ordovician stages is partly the result of the difficulties presented by diagenetic alteration of the primary isotopic signal (Veizer, 1989; Brand, 1991): the lowest values generally are considered closer to contemporary seawater values (Stille and Shields, 1997), since diagenesis may take place in more ^{87}Sr rich vadose porewaters (Veizer, 1989). However, even where this can be minimized or discounted, the scatter remains and is particularly pronounced in the Upper Ordovician (Brand et al., 2003; Shields et al., 2003; Brand, 2004) (Fig. 1).

There are several possible explanations for this. First, imprecise biostratigraphic correlation among the various sections studied, caused by pronounced provinciality (Candela, 2006) and continuous revision of biozones (Melchin et al., 2003), together with the coarse sampling intervals used, stratigraphically equates samples of different ages and obscures small-scale fluctuations in $^{87}Sr/^{86}Sr$ ratios through time. Precise stratigraphic placement is essential, but currently unobtainable

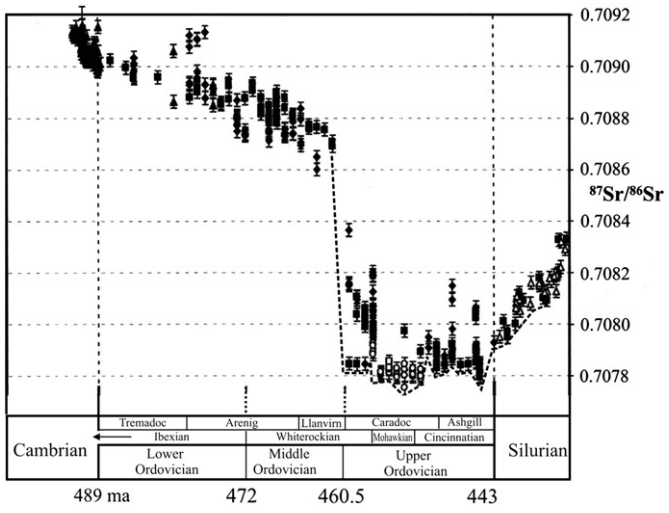

Fig. 1. Sr isotope curve for the Ordovician (after Shields et al. (2003); Fig. 8), based on apparently well-preserved brachiopods and carbonate components. Dotted line follows lowest ratios, considered the least altered.

(see Melchin et al., 2003; Sadler and Cooper, 2004) except with local biostratigraphy in individual sections (as here) where small-scale fluctuations in Sr isotope ratios may not be the result of diagenetic alteration but may truly reflect global climate cycles at the 1 to 1.5 Ma scale (Farrell et al., 1995) or even smaller scale cycles within the semi-isolated Taconic basin; though small-scale 100-kyr cycles proposed for the open oceans (Dia et al., 1992) have not been confirmed by later work (Henderson et al., 1994). The controlling fluxes are, however, capable of generating measurable changes in $^{87}Sr/^{86}Sr$ ratios in seawater over 10,000 year intervals (Veizer, 1989). Second, the partial isolation of epeiric seas, enclosed basins and retroarc basins, from the open ocean may also affect the isotope ratios (Allison and Wells, 2006; Fanton and Holmden, 2007; Brand et al., 2009; Holmden et al., 2010); though considerable amounts of freshwater (which usually has low strontium concentrations) must be added to an oceanic system to significantly affect the Sr isotope ratio (Reinhardt et al., 1998; Basu et al., 2001; Widerlund and Andersson, 2006). In a tropical latitude, like that of the northern Taconic basin, however, salinity may be significantly increased due to evaporation. For example, in the present tropical (~10°S) semi-isolated Gulf of Venezuela (average temperature 25 °C), with abundant surface freshwater input from Lake Maracaibo and rivers, salinities are about 29‰ to 37‰, increasing with depth (Ziegler, 1964), though there seems no data on its Sr-isotopic ratios. Anomalous Sr isotope ratios occur in the comparable semi-enclosed Gulf of California, northern Mexico (Tarnoff, 1986). Third, weathering of exposed carbonates of different ages can supply different Sr isotope ratios (Shields, 2007), which will affect the Sr isotope ratio of the contemporary ocean since carbonates are the major source of riverine strontium (Brass, 1976). In addition, extensive pressure solution (stylolitization) can supply dissolved Ca and Sr to groundwaters and this process begins at burial depths of 1–2 km (Verweij, 1993, p.34). Since the extensive Lower to Middle Ordovician carbonates have higher Sr isotope ratios (0.7088 and above) (Fig. 1), since some were buried to depths greater than 2 km during arc emplacement (Azmy et al., 2008), since even present outcrop carbonates are stylolitized, and since some were exposed by the Taconic orogeny during the Hirnantian sea-level drop (Ratcliffe et al., 1999), then this explanation has to be considered.

The intent of this paper is to present a well-defined Sr chemostratigraphy for the transition from the Upper Ordovician (Cincinnatian; Upper Katian–Lower Hirnantian) carbonate shelf to the clastic wedge in a section on the western shelf of the Appalachian basin by analyzing the shells of the articulate brachiopods *Paucicrura rogata* (Sardeson, 1892), a common opportunistic brachiopods which occur throughout the Upper Ordovician of eastern North America (Spafford et al., 1993). Unaltered brachiopods preserve original shell geochemistry back to the Upper Ordovician and, apart from conodonts, are the most reliable sources of unaltered isotopic compositions, especially compared to whole rock analyses (Popp et al., 1986; Qing et al., 1998; Brand, 2004) and by using one species we minimize any possible Sr variation from any vital effects, though modern marine calcareous taxa show no vital effects and have the same Sr-isotopic ratios as contemporary seawater (Reinhardt et al., 1999; Brand et al., 2003). By establishing the Sr isotope chemostratigraphy, we are able to describe detailed changes and fluctuations in the seawater Sr isotope composition of the western Upper Ordovician Taconic basin and relate them to paleoenvironmental changes during this interval of orogeny and transition to the latest Ordovician Hirnantian glaciation (Brenchley et al., 1994; Fortey and Cocks, 2005; Salzman and Young, 2005; Armstrong, 2007).

2. Geological setting

The Upper Ordovician northeastern passive margin of North America lay at about 25–30°S in tropical latitudes (Kent and Van der Voo, 1990) (Fig. 2A). Between the Appalachian and Michigan basins the Trenton Limestone Group forms an eastward deepening cool carbonate continental back-arc ramp succession (Brookfield, 1988; Brookfield and Brett, 1988; Cherns and Wheeley, 2007) which was transformed into a foredeep basin as the ramp collided with a succession of microcontinent fragments and magmatic arcs during the Taconic orogeny (Schoonmaker and Kidd, 2006; Zagorevski et al., 2006). Around 460 Ma (Middle to Upper Ordovician boundary), the ramp succession began to subside rapidly as Middle Ordovician volcanic arcs, microcontinents and ophiolites were emplaced in a geologically relatively short time span of ~20 Ma (Karabinos et al., 1998; Dewey, 2005; Hatcher et al., 2007; Ganis and Wise, 2008). Loading and flexure of the ramp, accompanied by clastic input from the collided microcontinents and arcs, led to subsidence and migration of slope and basin facies westwards together with increasingly juvenile clastic input from the Taconic uplifts to the east (Lehmann et al., 1995; Anderson and Samson, 2010) (Fig. 2B). Throughout the North American epeiric sea, a marked positive shift in ε_{Nd} in the lower Cincinnatian (Edenian) (Fig. 3) marks a shift from cratonic to Taconic sources as the Edenian transgression covered the craton (Fanton et al., 2002).

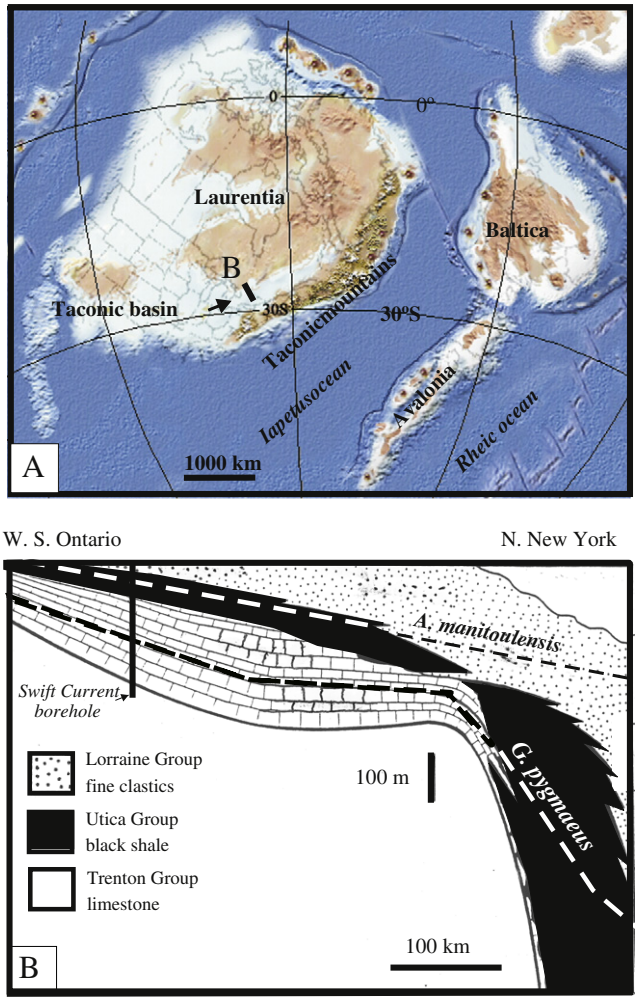

Fig. 2. A) Late Ordovician paleogeography (courtesy Ron Blakey), with location of cross-section. B) Cross-section of Upper Ordovician ramp from western southern Ontario to northern New York State showing location of the Swift Current borehole (modified from Lehmann et al. (1995)). Dotted lines are bases of respective graptolite zones (italics).

In Ontario, the deposition of this coarsening upwards clastic succession begins with the black anoxic shales of the Collingwood Formation, which pass up gradually into the silty oxic shales of the Blue Mountain Formation, in turn grading up into the Georgian Bay Formation, consisting of alternating laminated mudstones, siltstones and fine-grained storm-deposited sandstones, then bioclastic limestones and shales, capped by bioclastic dolomites (Byerley and

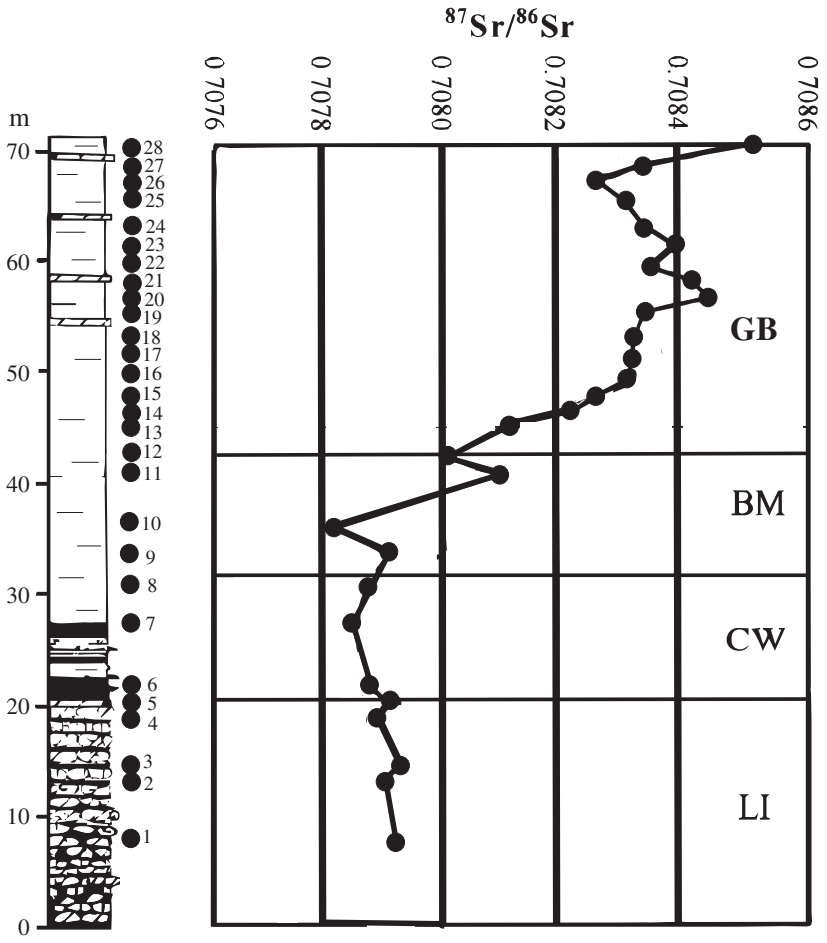

Fig. 3. Stratigraphic correlations of Upper Ordovician of southern Ontario. International stages from Webby et al. (2004), Xu Chen et al. (2006): North American stages and bentonite dates from Goldman et al. (1994; Sadler and Cooper (2004): graptolite zones from Goldman and Bergström (1997), Senior (1991); Ontario lithostratigraphy from Sandford (1961).

Coniglio, 1989; Kerr and Eyles, 1991) (Fig. 3). The Georgian Bay Formation passes upwards into the red Queenston Shale Formation deposited in prograding muddy deltaic to fluvial environments (Brogly et al., 1998). This shallowing upwards succession may be related to sea-level fall caused by the onset of the late Ordovician Hirnantian glaciation in North Africa (Villas et al., 2002) and/or the gradual filling in of the northern Taconic basin (English et al., 2006). The Queenston Shale is disconformably overlain by shoreline Whirlpool Sandstone of the early Silurian (Brett, 1990). The Collingwood Formation marks either a major rise in relative sea-level, a climatic change, or both, as anoxic black shales were spread over the carbonate ramp and shelf from the Appalachian trough far to the west (Brett et al., 2006). The overlying shallowing upwards succession has normal marine faunas only in the Blue Mountain Formation: the ones above have low diversity assemblages with suggestions of generally abnormal salinities, for example the scarcity, except in rare horizons, of stenohaline forms, such as crinoids and corals (Dyer, 1925; Haugh, 1979; Brogly et al., 1998). This change is consistent with the formation of Taconic island barriers between the main ocean and the retroarc basin (Faill, 1997).

The change from carbonate to black shale, though diachronous in New York, appears to be less so in Ontario, as it occurs within the global *G. pygmaeus* graptolite zone (Goldman and Bergström, 1997) (Fig. 3). Biostratigraphic zones and correlations, and chronostratigraphic ages however, are continually being revised for the Upper Ordovician (see LaPorte et al., 2009) and the carbon isotope stratigraphic correlations are debatable (Brenchley et al., 2003; Melchin and Holmden, 2006). It is beyond the scope of this article to discuss the integration of Upper Ordovician biostratigraphy, chemostratigraphy and chronostratigraphy. Here we use the Upper Ordovician time scale and correlations of Goldman et al. (1994) for Eastern North America and the recently established and dated International stages (Sadler and Cooper, 2004; Bergstrom et al., 2009) with bentonite dates from Tucker and McKerrow (1995) and Sharma et al. (2005). A recent analysis puts the Silurian/Hirnantian boundary at 443.41 Ma and the basal Hirnantian at 444.68 Ma (Sadler et al., 2009), a precision warranted neither by stratigraphic nor radiometric dating methods. These, however, are not much different from the International one used here. Sharma et al. (2005) considered their near plateau Ar–Ar age of 400–450 Ma to be too young compared to the age then determined for the global graptolitic *pygmaeus* zone (451–452 Ma from Webby et al, 2004) which hosted the bentonite. However, in fact, the *pygmaeus* zone ends the Katian stage with an upper boundary age of 445.6 ± 1.5 Ma, so the age is reasonable (Fig. 3). Despite the uncertainties in dating, the current stratigraphy suggests that the section above the Collingwood roughly corresponds with the Hirnantian (Bergstrom et al., 2009). Furthermore, our Sr-isotopic curve fits the general trend of the current Sr-isotopic curve for that interval (see p.000).

3. Methods

We sampled the uppermost Trenton carbonates (Lindsay Formation) and succeeding clastic units (Collingwood to Georgian Bay Formations) in a borehole (OGS 83-5, Manitoulin County, Howland

Township, Lot 6, Concession V; see Johnson et al., 1985) near the western margin of the Ontario–New York succession (Fig. 2). Samples were taken at intervals between 1 and a maximum of 5 m depending where *P. rogata* occurred (Fig. 4; Table 1) (Hannigan, 1997).

We examined thin sections of the core samples using transmitted light and cold cathodoluminescence microscopy to identify the state of preservation of the brachiopods, *P. rogata*. Samples of about 15 mg of shell material were removed from the cleaned rock surface using a needle and two 5 mg separates each were powdered for Sr-isotopic analysis and Sr and Mn trace element analysis. Powdered brachiopod material was dissolved in 4 M ultrapure nitric acid. $^{87}Sr/^{86}Sr$ measurements were made in dynamic multicollector mode on the VG Sector mass spectrometer at the University of Rochester. Each sample was measured in duplicate. Sr-isotopes were measured using the same procedures established for our laboratory at the University of Rochester (Basu et al., 1990). Analyses of National Bureau of Standards (NBS) reference material 987 ($n=12$) gave $^{87}Sr/^{86}Sr=0.710247\pm29$ (2σ, $\pm0.006\%$) during the course of these measurements. Mass fractionation was corrected using $^{86}Sr/^{88}Sr=0.1194$.

For Sr and Mn measurements we analyzed the carbonate samples with a VG Quadrupole Inductively Coupled Plasma Mass Spectrometer (ICP-MS) at the Union College facility in Schenectady, New York. We digested each 5 mg sample completely with 1 mL concentrated HNO_3 in tightly sealed 15 mL Teflon TFE screw-cap bomb by heating on a hot plate for 24 h. After evaporating to dryness under lamps, we prepared the final solutions by adding precisely 1 mL of the internal standard and diluting the sample to 100 mL with double distilled water. The composition of the internal standard was a 10 ppm solution of Ga, In, Cs, Bi and Re to correct instrumental drift for the ICP-MS analyses. We performed all sample preparation in the Class 100 clean room at the University of Rochester; all acids were ultrapure. At the time of these analyses we lacked a suitable matrix-matched standard for the shell material. We therefore used external calibration (5 standards covering the linear range of expected concentrations of Sr in 2% ultrapure nitric acid) and 2 check standards (12 ppb Sr and 125 ppm Sr). Check standards were analyzed between every 5 samples as unknowns. Standard error was calculated based on means of replicate analyses with errors less than 2%. Calibration was performed every 7 samples. Least squares regression coefficients were 0.9995 or better. All of the reported data are duplicate measures and therefore are a mean of two measures.

4. Results

The Sr and Mn concentrations and $^{87}Sr/^{86}Sr$ ratios of the samples are shown in Table 1 and a plot of the Sr contents and $^{87}Sr/^{86}Sr$ ratios are shown in Fig. 4. In hand specimens the brachiopods (*P. rogata*) appear well preserved, petrographically show little diagenetic overprint, and were non-luminescent under cathodoluminescence (Machel, 2000). Although the samples were non-luminescent, we compared the Sr and Mn composition to further explore the possibility of diagenetic overprint (Brand, 2004), which is crucial if we are to attribute any paleooceanographic significance to the isotope results. There is no systematic relationship between Mn and Sr

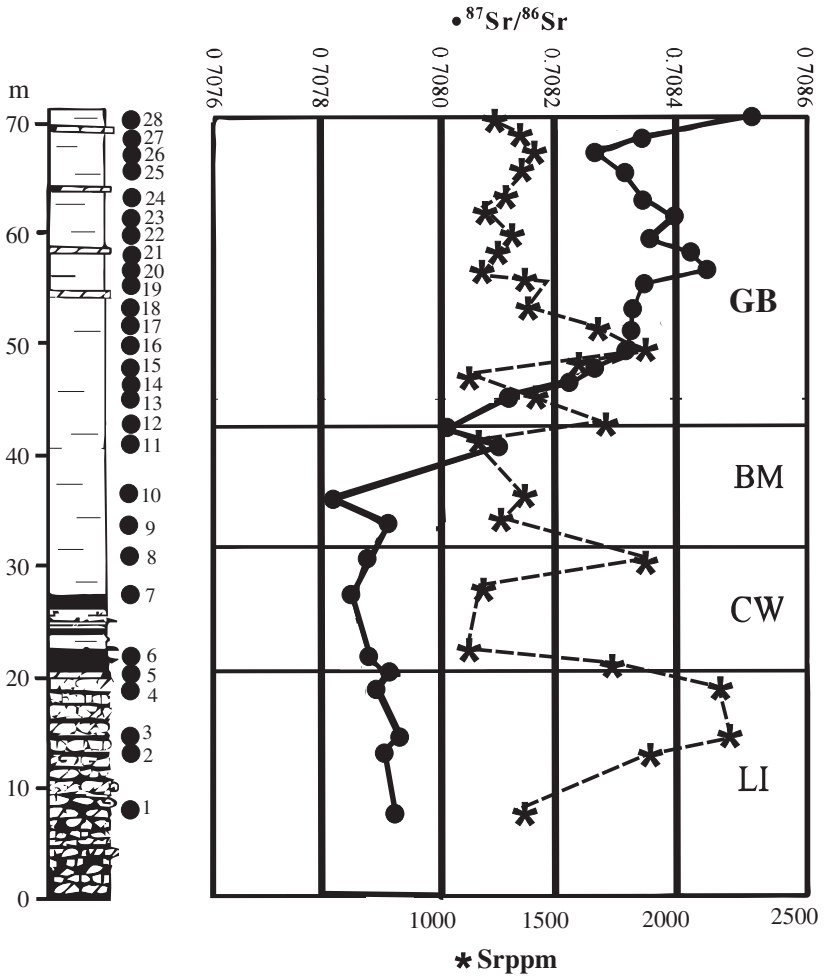

Fig. 4. Relevant section of the Swift Current core (83-5) based on Johnson et al. (1985) and personal examination with Sr isotope ratios (dots) and Sr ppm (stars) plotted. LI — Lindsay Formation; CW — Collingwood Formation; BM — Blue Mountain Formation; GB — Georgian Bay Formation.

indicating little or no diagenetic alteration, except in the Georgian Bay Formation where there is a weak tendency for inverse correlation of Sr and Mn which may reflect diagenesis (Fig. 5). The overall variability in the Mn/Sr ratios is within the range of modern brachiopods (see Shields et al., 2003, Fig. 4). Shallow water mid-latitude modern Terebratulid brachiopods have Mn contents up to 200 ppm at Sr contents of 1000 to 1200 ppm (Brand et al., 2003, Fig. 7). Therefore, we believe that the isotopic data recorded by these shells follow the ambient seawater conditions at the time of formation. Furthermore, the $^{87}Sr/^{86}Sr$/ Sr plot shows no relationships either (Fig. 6). Unfortunately, we did not analyze for Fe which would have provided further evidence of little or no diagenetic alteration (Brand and Veizer, 1980).

The Sr contents are between 1100 and 2243 ppm (Table 1), much higher than the secondary layer of modern brachiopods, which range from 450 (mid-latitude) to 1928 (temperate to arctic) ppm in shallow water environments with a cluster around 1000 ppm, and seem related to the temperature and salinity of the seawater (Brand et al., 2003). Older analyses of whole modern brachiopod shells, however, gave Sr contents between 800 and 2200 ppm, while Upper Ordovician brachiopods range from 297 to 2541 ppm (Popp et al., 1986) which fits the range here. Values of Upper Ordovician low-Mg calcite brachiopod shells range between 600 and 1500 ppm, but with a 1000 ppm average close to modern brachiopods (Steuber and Veizer, 2002).

The Sr-isotopic curve (Fig. 4) shows low values of between 0.70782 and 0.70792 from the Lindsay into the middle Blue Mountain Formations, *independent of lithology* and inferred environmental change from shallow carbonate ramp through anoxic conditions to synorogenic clastic input (Sharma et al., 2003). Commencing with the upper Blue Mountain Formation, there is a marked rise to values of above 0.7080 and this trend culminates in the value of 0.708507 for the topmost sample in the Georgian Bay Formation. The pattern in these values is the same as in the Upper Ordovician compilation of Shields et al. (2003), but shows a marked rise not seen in their data (Fig. 1). In fact, it shows similar variations to their compilation of Sr-isotopic data for all apparently well-preserved samples (Fig. 7), but reaches a value (0.708507) not reached until the end of the Silurian and unrecorded since the Middle Ordovician (Qing et al., 1998; Shields et al, 2003). Sr contents and $^{87}Sr/^{86}Sr$ ratios show a strong inverse correlation above the Collingwood Formation, though not below (Fig. 4).

5. Discussion

In normal seawater, Sr contents are lower in shallow mid-latitude and tropical waters, and higher in shallow temperate and polar waters

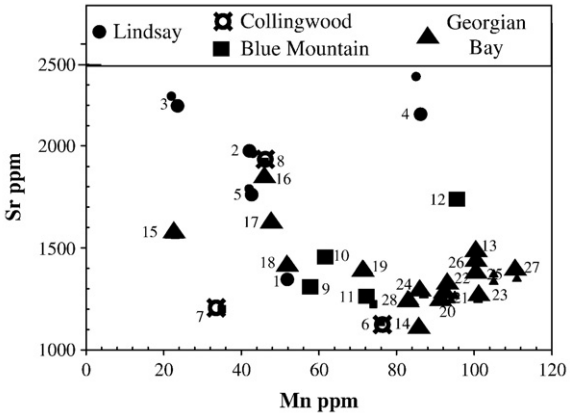

Fig. 5. Sr versus Mn plot for the brachiopods. The lack of relationship between Sr and Mn, and low Mn and high Sr concentrations are consistent with little to no diagenetic overprint. The plots lie within the field for modern brachiopods (Brand et al., 2003). Numbers at symbols are analysis numbers from Table 1.

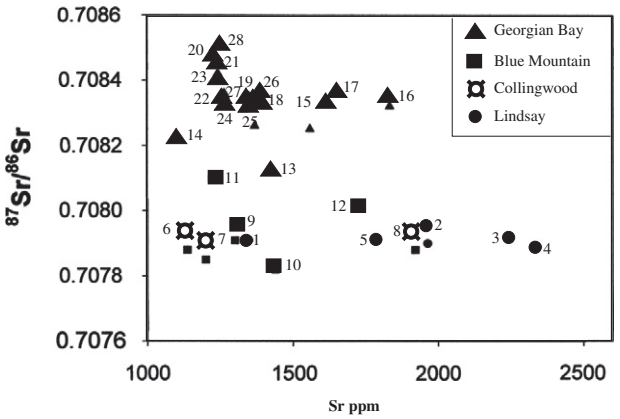

Fig. 6. Sr isotopic ratios versus Sr contents plot for the brachiopods. Numbers at symbols are analysis numbers from Table 1.

(Brand et al., 2003). This might explain the higher values in the upper Lindsay Formation which was deposited in the deeper, presumably colder waters of a deepening ramp, and the lower values in the Collingwood Formation, which may reflect a warmer interval.

The explanation for both the rapid fall in Sr isotope ratios at the beginning of the Upper Ordovician and the rapid rise at the end of the Upper Ordovician must be related to the balance between fluxes from radiogenic and non-radiogenic sources. The rapid decrease from the Middle to Upper Ordovician (Fig. 1) has been attributed to rapid marine transgression burying radiogenic continental sources, with increased flux from less radiogenic sources associated with more rapid Upper Ordovician sea-floor spreading and oceanic arc formation, resulting in low continental uplift and recycling rates, hydrothermal cycling and high rates of weathering of basic igneous rocks (Shields et al, 2003). The change, however, also corresponds to the emplacement of the large ophiolite nappes and oceanic arcs of eastern North America and elsewhere which took place near the Middle/Upper Ordovician boundary at 462 ± 3 Ma during relatively short period of arc-continent collisions which extend to Scandinavia and China (Castonguay et al.,

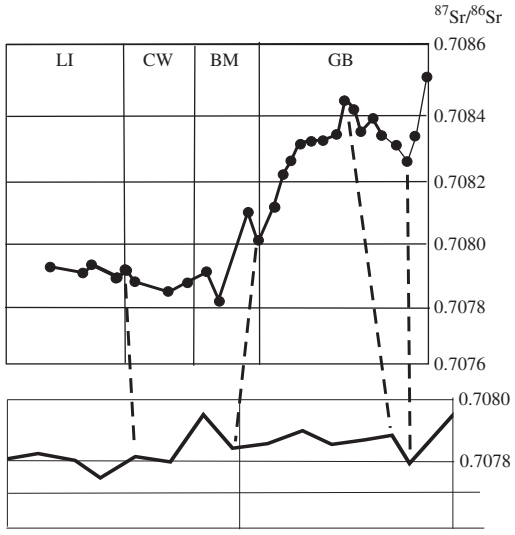

Fig. 7. Swift Current core Sr-isotopic ratios (top) compared to Katian–Hirnantian Sr-isotopic ratios (bottom) constructed from Fig. 8 of Shields et al (2003) using the lowest values of each sample suite. The difficulty of global stratigraphic correlation means that a stratigraphic thickness diagram for the core is juxtaposed with the Shields et al. (2003) time diagram for the global data. Dashed lines show possible correlations. The initials at the top refer to the Lindsay (LI), Collingwood (CW), Blue Mountain (BM) and Georgian Bay (GB) formations. Vertical $^{87}Sr/^{86}Sr$ scales are the same for both.

2001; Qiantao et al., 2001; Dewey, 2005). $^{87}Sr/^{86}Sr$ ratios of ophiolites are increased during oceanic hydrothermal alteration to around 0.7050 and arc volcanics (and derived sediments) are around 0.7036 (Alt and Teagle, 2000; Rad et al., 2007). In addition, since arcs contribute up to 73% of mantle derived strontium to the modern oceans (Allègre et al, 2010), these sources can account for the sharp drop. The rise in the Upper Ordovician may be explained by a reversal of these trends; marine regression during the onset of the Hirnantian glaciation, and uplift and erosion of continental rocks in the Appalachians during and after the Taconic orogeny (Karabinos et al., 1998; Qing et al., 1998). The detrital zircons in the Upper Ordovician Taconic retroarc sediments are derived from Precambrian, not Paleozoic, sources indicating erosion of basement allochthons (Hatcher et al., 2007). In our study the Sr-isotopic ratio increase takes place earlier than in the Shields et al. (2003) compilation, above the major Collingwood Formation black shale unit (Oceanic Anoxic Event) during deposition of the shallowing upwards succession of clastics derived from the rising Taconic allochthons to the east. Nevertheless, the pattern of our $^{87}Sr/^{86}Sr$ follows the Shields et al. (2003) curve indicating that it reflects contemporary seawater changes; but the greatly increased $^{87}Sr/^{86}Sr$ ratios for the Georgian Bay Formation suggest much greater continental influence from the rising Taconic orogen to the east (including erosion of tectonically exposed earlier Ordovician carbonates with their higher Sr isotope ratios) and that the Taconic retroarc basin water was not completely equilibrated with the open ocean in its geochemistry.

The short reversal with less radiogenic $^{87}Sr/^{86}Sr$ ratios within the upper Georgian Bay (Fig. 6, between dashed lines in GB) cannot yet be explained, though it may relate to the youngest Ordovician arc accretion (~450 Ma) in central Newfoundland (Zagorevski et al., 2006), or to a marine transgression: the topmost Georgian Bay has indications of increased salinities as it contains coral and stromatoporoid bioherms (Byerley and Coniglio, 1989). Sharp changes in $^{87}Sr/^{86}Sr$ ratios can be caused by variations in river input, particularly if Sr concentrations are higher than normal due to carbonate rock solution. For example, the sharp rise in $^{87}Sr/^{86}Sr$ ratios in the Black Sea between 16.5 and 14.8 ky BP is attributed to increased runoff in the transition from a cold to a warm phase (Bahr et al., 2008).

6. Conclusions

$^{87}Sr/^{86}Sr$ ratios and minor element analyses of stratigraphically closely spaced samples were made from a single brachiopod species from the Cincinnatian (Upper Ordovician) shelf of Ontario, the landward side of a retroarc basin formed during arc-continent collisions which began at the beginning of the Upper Ordovician. These analyses indicate that the $^{87}Sr/^{86}Sr$ ratios preserved a primary seawater signal. The close spacing allows a detailed Sr-isotopic curve to be constructed which, although it fits the pattern for the equivalent strata elsewhere, shows much more detail and has much higher $^{87}Sr/^{86}Sr$ ratios, particularly in the upper beds. The rise in ratios begins with the onset of shallowing in our section and at a level equivalent to the start of the late Ordovician Hirnantian ice age and thus may reflects eustatic drop in sea-level as elsewhere, though the much higher values in Ontario also suggest increased erosion from Taconic mountains to the east and incomplete mixing with the open ocean. Since we do not know the volume of the Taconic basin only qualitative estimates of paleosalinity are possible from the faunas. Calculations of possible paleosalinities, like those done in the Baltic Sea Holocene from Sr isotope mixing calculations, are not possible (Widerlund and Andersson, 2006). The detail within the overall pattern can also not yet be satisfactorily explained. More detailed analyses of Neogene sediments from a DSDP core show that small-scale fluctuations in $^{87}Sr/^{86}Sr$ ratios can be related to glacial kyr cycles (Farrell et al., 1995): such analyses should also be tried for the Upper Ordovician, especially since Milankovitch cycles are claimed, from other methods, to occur in our core sediments (Hannigan, 1997) and elsewhere (Williams, 1991).

Acknowledgements

For support, MB thanks Academia Sinica and ARB thanks US-NSF. We also thank the Ontario Geological Survey for access to the Swift Current core, and Tom Algeo and Carl Brett for comments on earlier versions of the manuscript, and two anonymous referees for careful and constructive comments after submission.

References

Allègre, C.J., Louvat, P., Gaillardet, J., Meynadier, L., Rad, S., Capmas, F., 2010. The fundamental role of island arc weathering in the oceanic Sr isotope budget. Earth and Planetary Science Letters 292, 51–56.
Allison, P.A., Wells, M.R., 2006. Circulation in large ancient epicontinental seas: what was different and why? Palaios 21, 513–515.
Alt, J.C., Teagle, D.A.H., 2000. Hydrothermal alteration and fluid fluxes in ophiolites and oceanic crust. Geological Society of America Special Paper 349, 273–282.
Anderson, C.B., Samson, S.D., 2010. Temporal changes in Nd isotopic composition of sedimentary rocks in the Sevier and Taconic foreland basins: increasing influence of juvenile sources. Geology 23, 983–986.
Andersson, P.S., Wasserburg, G.J., Ingri, J., 1992. The sources and transport of Sr and Nd isotopes in the Baltic Sea. Earth and Planetary Science Letters 113, 459–472.
Armstrong, H.A., 2007. On the cause of the Ordovician glaciation. In: Haywood, W.M., Gregory, A.M., Schmidt, D.N. (Eds.), Deep-time Perspectives on Climate Change: Marrying the Signal from Computer Models and Biological Proxies. The Geological Society, London, UK, pp. 101–121.
Azmy, K., Lavoie, D., Knight, I., Chi, Guoxiang, 2008. Dolomitization of the Lower Ordovician Aguathuna Formation carbonates, Port au Port Peninsula, western Newfoundland, Canada: implication for a hydrocarbon reservoir. Canadian Journal of Earth Sciences 45, 795–813.
Bahr, A., Lamy, F., Arz, H.W., Major, C., Kwiecien, O., Wefer, G., 2008. Abrupt changes of temperature and water chemistry in the late Pleistocene and early Holocene Black Sea. Geochemistry, Geophysics, Geosystems 9. doi10.1029/2007GC001683.
Basu, A.R., Sharma, M., DeCelles, P.G., 1990. Nd, Sr-isotopic provenance and trace element geochemistry of Amazonian Foreland Basin fluvial sands, Bolivia and Peru: implications for ensialic Andean Orogeny. Earth and Planetary Science Letters 100, 1–17.
Basu, A.R., Jacobsen, S.B., Poreda, R.J., Dowling, C.B., Aggarwal, P.K., 2001. Large groundwater strontium flux to the oceans from the Bengal Basin and the marine strontium isotope record. Science 293, 1470–1473.
Bergstrom, S.M., Che, Xu., Guttiérrez-Marco, J.C., Dronov, A., 2009. The new chronostratigraphic classification of the Ordovician System and its relations to major regional series and stages and to $\delta^{13}C$ chemostratigraphy. Lethaia 42, 97–107.
Bradley, D.C., 1989. Taconic plate kinematics as revealed by foredeep stratigraphy, Appalachian Orogen. Tectonics 8, 1037–1049.
Brand, U., 1991. Strontium isotope diagenesis of biogenic aragonite and low-Mg calcite. Geochemica et Cosmochemica Acta 55, 505–513.
Brand, U., 2004. Carbon, oxygen and strontium isotopes in Paleozoic carbonate components: an evaluation of original seawater-chemistry proxies. Chemical Geology 204, 23–44.
Brand, U., Veizer, J., 1980. Chemical diagenesis of a multicomponent carbonate system: 1.Trace elements. Journal of Sedimentary Petrology 50, 155–264.
Brand, U., Logan, A., Hiller, N., Richardson, J., 2003. Geochemistry of modern brachiopods: applications and implications for oceanography and paleoceanography. Chemical Geology 198, 305–334.
Brand, U., Tazawa, Juni-ichi, Sano, Hiroyoshi, Azmy, K., Lee, Xinqing, 2009. Is mid–late Paleozoic ocean-water chemistry coupled with epeiric seawater isotope records? Geology 37, 823–826.
Brass, G.W., 1976. The variation of the marine $^{87}Sr/^{86}Sr$ ratio during Phanerozoic time: interpretation using a flux model. Geochimica et Cosmochimica Acta 40, 721–730.
Brenchley, P.J., Marshall, J.D., Carden, G.A.F., Robertson, D.B.R., Long, D.G.F., Meidla, T., Hints, L., Anderson, T., 1994. Bathymetric and isotopic evidence for a short-lived Late Ordovician glaciation in a greenhouse period. Geology 22, 295–298.
Brenchley, P.J., Carden, G.A., Hints, L., Kaljo, D., Marshall, J.D., Martma, T., Meidla, T., Nõlvak, J., 2003. High-resolution stable isotope stratigraphy of Upper Ordovician sequences: constraints on the timing of bioevents and environmental changes associated with mass extinction and glaciation. Geological Society of America Bulletin 115, 89–104.
Brett, C.E., 1990. Sequences, cycles, and basin dynamics in the Silurian of the Appalachian foreland basin. Sedimentary Geology 69, 1–52.
Brett, C.E., Allison, P.A., Tsujita, C.J., Soldani, D., Moffat, H.A., 2006. Sedimentology, taphonomy, and paleoecology of meter-scale cycles from the Upper Ordovician of Ontario. Palaios 21, 530–547.
Brogly, P.J., Martini, I.P., Middleton, G.V., 1998. The Queenston Formation: shale dominated, mixed terrigenous-carbonate deposits of Upper Ordovician, semiarid, muddy shores in Ontario, Canada. Canadian Journal of Earth Sciences 35, 702–719.
Brookfield, M.E., 1977. The emplacement of giant ophiolite nappes 1. Mesozoic–Cenozoic examples. Tectonophysics 37, 247–303.
Brookfield, M.E., 1988. A mid-Ordovician temperate carbonate shelf ? The Black River and Trenton Limestone groups of southern Ontario, Canada. Sedimentary Geology 60, 137–153.

Brookfield, M.E., 1993. The interrelations of post-collision tectonism and sedimentation in Central Asia. Special Publications of the International Association of Sedimentologists 20, 13–35.
Brookfield, M.E., Brett, C.E., 1988. Paleoenvironments of the Mid-Ordovician (Upper Caradoc) Trenton limestones of southern Ontario, Canada: storm sedimentation on a shoal-basin-shelf model. Sedimentary Geology 57, 185–198.
Burke, W.H., Dennison, R.E., Hetherington, E.A., Koepnick, R.B., Nelson, H.F., Otto, J.B., 1982. Variation of seawater $^{87}Sr/^{86}Sr$ throughout Phanerozoic time. Geology 10, 516–519.
Byerley, M., Coniglio, M., 1989. Stratigraphy and sedimentology of the Upper Ordovician Georgian Bay Formation, Manitoulin Island and Bruce Peninsula. Ontario Geological Survey Miscellaneous Paper 143, 227–237.
Candela, Y., 2006. Statistical comparisons of late Caradoc (Ordovician) brachiopod faunas around the Iapetus Ocean, and terranes located around Australia, Kazakhstan and China. Geodiversitas 23, 433–446.
Capo, R.C., DePaolo, D.J., 1992. EOS. Transactions of the American Geophysical Union 73, 272.
Castonguay, S., Ruffet, G., Tremblay, A., Féraud, G., 2001. Tectonometamorphic evolution of the southern Quebec Appalachians: $^{40}Ar/^{39}Ar$ evidence for Ordovician crustal thickening and Silurian exhumation of the internal Humber zone. Geological Society of America Bulletin 113, 144–160.
Chen, Xu., Rong, Jiayu, Fan, Junxuan, Zhan, Renbin, Mitchell, C.E., Harper, D.A.T., Melchin, M.J., Peng, Ping'an, Finney, S.C., Wang, Xiaofeng, 2006. The global boundary stratotype section and point (GSSP) for the base of the Hirnantian Stage (the uppermost of the Ordovician System). Episodes 29, 183–196.
Cherns, L., Wheeley, J.R., 2007. A pre-Hirnantian (Late Ordovician) interval of global cooling — the Boda event re-assessed. Palaeogeography, Palaeoclimatology, Palaeoecology 251, 449–460.
Dennison, R.E., Koepnick, R.B., Burke, W.H., Hetherington, E.A., 1998. Construction of the Cambrian and Ordovician seawater $^{87}Sr/^{86}Sr$ curve. Chemical Geology 152, 325–340.
DePaolo, D.J., 1986. Detailed record of the Neogene Sr isotopic evolution of seawater from DSDP Site 590B. Geology 14, 103–106.
Dewey, J.F., 2005. Orogeny can be very short. Proceedings of the National Academy of Sciences 102, 15286–15293.
Dia, A.N., Cohen, A.S., O'Nions, R.K., Shackleton, N.J., 1992. Seawater Sr isotope variation over the past 300 kyr and influence of global climate cycles. Nature 256, 786–788.
Dyer, W.S., 1925. The paleontology of the Credit River section. Ontario Department of Mines Annual Report 32 (7), 47–88.
Elderfield, H., 1986. Strontium isotope stratigraphy. Palaeogeography, Palaeoclimatology, Palaeoecology 57, 71–90.
English, A.M., Landing, E., Baird, G.C., 2006. Snake Hill — reconstructing eastern Taconic foreland basin litho- and biofacies from a giant mélange block in eastern New York, USA. Palaeogeography, Palaeoclimatology, Palaeoecology 242, 201–213.
Faill, R.T., 1997. A geologic history of the north-central Appalachians: Part 1, Orogenesis from the Mesoproterozoic through the Taconic orogeny. American Journal of Science 297, 551–619.
Fanton, K.C., Holmden, C., 2007. Sea-level forcing of carbon isotope excursions in epeiric seas: implications for chemostratigraphy. Canadian Journal of Earth Sciences 44, 807–818.
Fanton, K.C., Holmden, C., Nowlan, G.S., Haidl, F.M., 2002. $^{143}Nd/^{144}Nd$ and Sm/Nd stratigraphy of Upper Ordovician epeiric sea carbonates. Geochimica et Cosmochimica Acta 66, 241–255.
Farrell, J.W., Clemens, S., Gromet, L.P., 1995. Improved chronostratigraphic reference curve of the late Neogene seawater $^{87}Sr/^{86}Sr$. Geology 23, 403–406.
Flecker, R., Ellamb, R.M., 2006. Identifying Late Miocene episodes of connection and isolation in the Mediterranean–Paratethyan realm using Sr isotopes. Sedimentary Geology 188–189, 189–203.
Fortey, R.A., Cocks, L.R.M., 2005. Late Ordovician global warming — the Boda event. Geology 33, 405–408.
France-Lanord, C., Derry, L., Michard, A., 1993. Evolution of the Himalaya since Miocene time: isotopic and sedimentological evidence from the Bengal Fan. Geological Society Special Publication 74, 603–621.
Ganis, G., Wise, D.U., 2008. Taconic events in Pennsylvania: datable phases of a 20 M.Y. orogeny. American Journal of Science 308, 167–183.
Goldman, D., Bergström, S.M., 1997. Late Ordovician graptolites from the North American Midcontinent. Palaeontology 40, 965–1010.
Goldman, D., Mitchell, C.E., Bergström, S.M., Delano, J.W., Tice, S., 1994. K-bentonites and graptolite biostratigraphy in the Middle Ordovician of New York State and Quebec: a new chronostratigraphic model. Palaios 9, 124–143.
Gustafsson, E.O., Omstedt, A., 2009. Sensitivity of Baltic Sea deep water salinity and oxygen concentration to variations in physical forcing. Boreal Environment Research 14, 18–30.
Hannigan, R.E., 1997. Trace and major elements in sedimentary and igneous processes: REE geochemistry of black shales and MORB and major element chemical variation in plume-generated basalts. Ph.D. Dissertation, University of Rochester, New York.
Harris, N., 1995. Significance of weathering Himalayan metasedimentary rocks and leucogranites for the Sr isotope evolution of seawater during the early Miocene. Geology 23, 795–798.
Hatcher Jr., R.D., Bream, B.R., Merschat, A.J., 2007. Tectonic map of the southern and central Appalachians: a tale of three orogens and a complete Wilson cycle. Geological Society of America Memoir 200, 595–632.
Haugh, B.N., 1979. Late Ordovician channel-dwelling crinoids from Southern Ontario, Canada. American Museum Novitiates 2665, 1–25.
Henderson, G.M., Martel, D.J., O'Nions, R.K., Shackleton, N.J., 1994. Evolution of seawater $^{87}Sr/^{86}Sr$ over the last 400 ka: the absence of glacial/interglacial cycles. Earth and Planetary Science Letters 128, 643–651.
Hess, J., Bender, M.L., Schilling, J.-G., 1986. Evolution of the ratio of strontium-87 to strontium-86 in Seawater from Cretaceous to present. Science 231, 979–984.
Holmden, C., Creaser, R.A., Muehlenbachs, K., Leslie, S.A., Bergström, S.M., 2010. Isotopic evidence for geochemical decoupling between ancient epeiric seas and bordering oceans: implications for secular curves. Geology 26, 567–570.
Jacobsen, S.B., Wasserburg, G.J., 1979. Nd and Sr isotopic study of the Bay of Islands ophiolite complex and the evolution of the source of midocean ridge basalts. Journal of Geophysical Research 84, 7429–7445.
Johnson, M.D., Russell, D.J., Telford, P.G., 1985. Oil Shale assessment project: drillholes for regional correlation 1983/84. Ontario Geological Survey Open File Report 5565, 1–49.
Jones, C.E., Jenkyns, H.C., 2001. Seawater strontium isotopes, oceanic anoxic events, and seafloor hydrothermal activity in the Jurassic and Cretaceous. American Journal of Science 301, 112–149.
Karabinos, P., Samson, S.D., Hepburn, J.C., Stoll, H.M., 1998. The Taconian orogeny in New England: collision between Laurentia and the Shelburne Falls arc. Geology 26, 215–218.
Kawahata, H., Nohara, M., Ishuzuka, H., Hasebe, S., Chiba, H., 2001. Sr isotope geochemistry and hydrothermal alteration of the Oman ophiolite. Journal of Geophysical Research 106B, 11083–11099.
Kent, D.V., Van der Voo, R., 1990. Palaeozoic palaoegeography from palaeomagnetism of the Atlantic-bordering continents. Geological Society of London Memoir 12, 49–56.
Kerr, M., Eyles, N., 1991. Storm-deposited sandstones (tempestites) and related ichnofossils of the Late Ordovician Georgian Bay Formation, southern Ontario. Canadian Journal of Earth Sciences 28, 266–282.
Koepnick, R.B., Burke, W.H., Denison, R.E., Hetherington, E.A., Nelson, H.F., Otto, J.B., Waite, L.E., 1985. Chemical Geology (Isotope Geoscience Section) 58, 55–81.
LaPorte, D.F., Holmden, C., Patterson, W.P., Loxton, J.D., Melchin, M.J., Mitchell, C.E., 2009. Local and global perspectives on carbon and nitrogen cycling during the Hirnantian glaciation. Palaeogeography, Palaeoclimatology, Palaeoecology 276, 182–195.
Lehmann, D., Brett, C.E., Cole, R., Baird, G., 1995. Distal sedimentation in a peripheral foreland basin: Ordovician black shales and associated flysch of the western Taconic foreland, New York State and Ontario. Geological Society of America Bulletin 107, 708–724.
Machel, H.G., 2000. Application of cathodoluminescence to carbonate diagenesis. In: Pagel, M., Barbin, V., Blanc, P., Ohnenstetter, D. (Eds.), Cathodoluminescence in Geosciences. Springer Verlag, Berlin Heidelberg New York, pp. 271–302.
Maslowski, W., Walczowski, W., 2002. Circulation of the Baltic Sea and its connection to the Pan-Arctic region — a large scale and high-resolution modeling approach. Boreal Environment Research 7, 319–325.
McArthur, J.M., 1994. Recent trends in strontium isotope stratigraphy. Terra Nova 6, 331–358.
McArthur, J.M., Howarth, R.J., Bailey, T.R., 2001. Strontium isotope stratigraphy: LOWESS version 3: best fit to the marine isotope curve for 0–509 Ma and accompanying look-up table for deriving numerical age. Journal of Geology 109, 155–170.
Melchin, M.J., Holmden, C., 2006. Carbon isotope chemostratigraphy in Arctic Canada. Sea-level forcing of carbonate platform weathering and implications for global correlation and sea-level change. Palaeogeography, Palaeoclimatology, Palaeoecology 234, 186–200.
Melchin, M.J., Holmden, C., Williams, S.H., 2003. Correlation of graptolite biozones, chitinozoan biozones, and carbon isotope curves through the Hirnantian. Instituto Superior de Correlación Geológica (Tucman, Argentina). Serie Correlación Geológica 17, 101–104.
Nelson, K.D., Casey, J.F., 1979. Ophiolitic detritus in the Upper Ordovician flysch of Notre Dame Bay and its bearing on the tectonic evolution of western Newfoundland. Geology 7, 27–31.
Palmer, M.R., Edmond, J.M., 1989. The strontium isotope budget of the modern ocean. Earth and Planetary Science Letters 92, 11–26.
Palmer, M.R., Elderfield, H., 1985. Sr isotope composition of sea water over the last 75 Myr. Nature 314, 526–528.
Popp, B.N., Anderson, T.F., Sandberg, P.A., 1986. Brachiopods as indicators of original isotopic compositions in some Paleozoic limestones. Geological Society of America Bulletin 97, 1262–1269.
Prinsberg, S.J., 1986. The circulation pattern and current structure of Hudson Bay. In: Martini, I.P. (Ed.), Canadian Inland Seas. Elsevier, Amsterdam, pp. 187–216.
Purdy, E.G., 2008. Comparison of taxonomic diversity, strontium isotope and sea-level patterns. International Journal of Earth Science 97, 651–664.
Qiantao, B., Leiming, Y., Shufen, S., Xiaoquan, L., Pospelov, I., Astrakhantsev, O., Chamov, N., 2001. Discovery of Ordovician acritarchs in Buqingshan ophiolite complex, East Kunlun. Mountains and its significance. Chinese Science Bulletin 46, 342–346.
Qing, H., Barnes, C.R., Buhl, D., Veizer, J., 1998. The strontium isotopic composition of Ordovician and Silurian conodonts: relationships to geological events and implications for coeval seawater. Geochimica et Cosmochimica Acta 62, 1721–1733.
Rad, S., Allègre, C.J., Louvat, P., 2007. Hidden erosion on volcanic islands. Earth and Planetary Science Letters 262, 109–124.
Ratcliffe, N.M., Harris, A.G., Walsh, G.J., 1999. Tectonic and regional metamorphic implications of the discovery of Middle Ordovician conodonts in cover rocks east of the Green Mountain massif, Vermont. Canadian Journal of Earth Sciences 36, 371–382.
Reinhardt, E.G., Stanley, D.J., Patterson, R.T., 1998. Strontium isotopic–paleontological method as a high-resolution paleosalinity tool for lagoonal environments. Geology 26, 1003–1006.
Reinhardt, E.G., Blenkinsop, J., Patterson, R.T., 1999. Assessment of Sr isotope vital effects ($^{87}Sr/^{86}Sr$) in marine taxa from Lee Stocking Island, Bahamas. Geo-Marine Letters 18, 241–246.

Richter, F.M., Rowley, D.B., DePaolo, D.J., 1992. Sr isotope evolution of seawater: the role of tectonics. Earth and Planetary Science Letters 109, 11–23.
Ruppel, S.C., James, E.W., Barrock, J.E., Nowland, G., Uyeno, T.T., 1996. High resolution $^{87}Sr/^{86}Sr$ chemostratigraphy of the Silurian: implications for event correlation and strontium flux. Geology 24, 831–834.
Sadler, P.M., Cooper, R.A., 2004. Calibration of the Ordovician timescale. In: Webby, B.D., Paris, F., Droser, M.L., Percival, I.G. (Eds.), The Great Ordovician Biodiversification Event. Columbia University Press, New York, pp. 48–51.
Sadler, P.M., Cooper, R.A., Melchin, M.A., 2009. High-resolution early Paleozoic (Ordovician–Silurian) time scales. Geological Society of America Bulletin 121, 887–906.
Salzman, M.R., Young, S.A., 2005. Long-lived glaciation in the Late Ordovician? Isotopic and sequence stratigraphic evidence from western Laurentia. Geology 33, 109–112.
Sandford, B.V., 1961. Subsurface stratigraphy of Ordovician rocks in southwestern Ontario. Geological Survey of Canada Paper 60–26, 1–54.
Sardeson, F.W., 1892. The range and distribution of the lower Silurian faunas of Minnesota with descriptions of some new species. Bulletin of the Minnesota Academy of Natural Science 3, 326–343.
Schoonmaker, A., Kidd, W.S.F., 2006. Evidence for a ridge subduction event in the Ordovician rocks of north-central Maine. Geological Society of America Bulletin 118, 897–912.
Senior, S.J.H., 1991. A new species of graptoloid, *Dicellograptus uncatus* n.sp. from the Blue Mountain Formation of southern Ontario, Canada. Canadian Journal of Earth Science 28, 822–826.
Sharma, S., Dix, G.R., Riva, J.F.V., 2003. Late Ordovician platform foundering, its paleoceanography and burial, as preserved in separate (eastern Michigan basin, Ottawa embayment) basins, southern Ontario. Canadian Journal of Earth Sciences 40, 135–148.
Sharma, S., Dix, G.R., Villeneuve, M., 2005. Petrology and potential tectonic significance of a K-bentonite in a Taconian shale basin (eastern Ontario, Canada), northern Appalachians. Geological Magazine 142, 145–158.
Shields, G.A., 2007. A normalized seawater strontium isotope curve: possible implications for Neoproterozoic–Cambrian weathering rates and the further oxygenation of the Earth. eEarth 2, 35–42.
Shields, G.A., Carden, G.A.F., Veizer, J., Meidla, T., Rong, Jia-Yu, Li, Rong-Yu, 2003. Sr, C, and O isotope geochemistry of Ordovician brachiopods: a major isotopic event around the Middle–Late Ordovician transition. Geochimica et Cosmochimica Acta 67, 2005–2025.
Spafford, C.A., Cisne, J.L., Railsback, B., Anderson, T.F., 1993. Punctal density in the Ordovician orthide brachiopod *Paucicrura rogata*: anatomical and paleoenvironmental variation. Lethaia 26, 17–24.
Spooner, E.T.C., 1976. The Strontium isotopic composition of seawater, and seawater–oceanic crust interactions. Earth and Planetary Science Letters 31, 167–174.
Steuber, T., Veizer, J., 2002. Phanerozoic record of plate tectonic control of seawater chemistry and carbonate sedimentation. Geology 30, 1123–1126.
Stille, P., Shields, G.A., 1997. Radiogenic isotope geochemistry of sedimentary and aquatic systems. Lecture Notes in Earth Science, 68. Springer Verlag, pp. 389–410.
Stille, P., Chaudhuri, S., Kharaka, Y.K., Clauer, N., 1992. Neodymium, strontium, oxygen and hydrogen isotopic compositions of waters in present and past oceans: a review. In: Clauer, N., Chaudhuri, S. (Eds.), Isotopic Signatures and Sedimentary Records. Springer-Verlag, Berlin, pp. 389–410.
Tarnoff, S., 1986.Anomalous Strontium Isotopic Compositions in Recent Seawater and Marine Carbonates from the Gulf of California. Unpub. MSc, California State University, Los Angeles.
Tucker, R.D., McKerrow, W.S., 1995. Early Paleozoic chronology: a review in light of new U–Pb zircon ages from Newfoundland and Britain. Canadian Journal of Earth Sciences 32, 368–379.
Vasiliev, I., Reichart, G.-J., Davies, G.R., Krijgsman, W., Stoica, M., 2010. Strontium isotope ratios of the Eastern Paratethys during the Mio–Pliocene transition; implications for interbasinal connectivity. Earth and Planetary Science Letters 292, 123–131.
Veizer, J., 1989. Strontium isotopes in seawater through time. Annual Review of Earth and Planetary Sciences 17, 141–167.
Veizer, J., Compston, W., 1974. Composition of seawater during the Phanerozoic. Geochimica et Cosmochimica Acta 38, 1461–1484.
Veizer, J., Ala, D., Azmy, K., Bruckschen, P., Buhl, D., Bruhn, F., Carden, G.A.F., Diener, A., Ebneth, S., Godderis, Y., Jasper, T., Korte, C., Pawellek, F., Podlaha, O.G., Strauss, H., 1999. $^{87}Sr/^{86}Sr$, $\delta^{13}C$ and $\delta^{18}O$ evolution of Phanerozoic seawater. Chemical Geology 161, 59–88.
Verweij, J.M., 1993. Hydrocarbon Migration Systems Analysis. Elsevier, Amsterdam.
Villas, E., Vennin, E., Álvaro, J.J., Hammann, W., Herrera, Z.A., Piovano, E.L., 2002. The late Ordovician carbonate sedimentation as a major triggering factor of the Hirnantian glaciation. Bulletin de la Société Géologique de France 173, 569–578.
Webby, B.D., Cooper, R.A., Bergström, S.M., Paris, F., 2004. Stratigraphic framework and time slices. In: Webby, B.D., Paris, F., Droser, M.L., Percival, I.G. (Eds.), The Great Ordovician Biodiversification Event. Columbia University Press, New York, pp. 41–47.
Widerlund, A., Andersson, P.S., 2006. Strontium isotopic composition of modern and Holocene mollusk shells as a palaeosalinity indicator for the Baltic Sea. Chemical Geology 232, 54–66.
Williams, H., 1975. Structural succession, nomenclature, and interpretation of transported rocks in Western Newfoundland. Canadian Journal of Earth Sciences 12, 1874–1894.
Williams, G.E., 1991. Milankovitch-band cyclicity in bedded halite deposits contemporaneous with Late Ordovician–Early Silurian glaciation, Canning Basin, Western Australia. Earth and Planetary Science Letters 103, 143–155.
Winter, B.L., Clark, D.L., Johnson, C.M., 1997. Late Cenozoic Sr isotope evolution of the Arctic Ocean: constraints on water mass exchange with the lower latitude ocean. Deep-sea Research part 2 (44), 1531–1542.
Young, S.A., Saltzman, M.A., Foland, K.A., Linder, J.S., Kump, L.R., 2009. A major drop in seawater $^{87}Sr/^{86}Sr$ during the Middle Ordovician (Darriwilian): links to volcanism and climate. Geology 37, 951–954.
Zagorevski, A., Rogers, N., Van Staal, C.R., McNicoll, V.M., Lissenberg, C.J., Valverde-Vaquero, P., 2006. Lower to Middle Ordovician evolution of peri-Laurentian arc and backarc complexes in Iapetus: constraints from the Annieopsquotch accretionary tract, central Newfoundland. Geological Society of America Bulletin 118, 324–342.
Ziegler, J.M., 1964. The hydrography and sediments of the Gulf of Venezuela. Limnology and Oceanography 9, 397–411.